

## Enhancement of rate of heat transfer in HCCI engine with induction induced swirl and under varying compression ratios and boost pressures<sup>†</sup>

T. Karthikeya Sharma<sup>\*</sup>, G. Amba Prasad Rao and K. Madhu Murthy

*Department of Mechanical Engineering, NIT Warangal, 506004(T.S), India*

(Manuscript Received March 26, 2015; Revised June 3, 2015; Accepted June 3, 2015)

### Abstract

Better fuel economy and lower NOx and PM emissions are the two major issues perplexing the researchers as well as new engine developers. Of late a new combustion concept- HCCI has gained popularity in this direction. Low combustion chamber temperatures favor low NOx emission formation. An attempt is made to study the effect of induction induced swirl in enhancing the rate of heat transfer to attain low in-cylinder temperatures favoring low NOx emissions formation. In this regard a computational study is undertaken in analyzing the heat distribution to the engine parts in HCCI mode of combustion under four swirl ratios and operating parameters. Extensive numerical study is carried out on a single cylinder 1.6 L, reentrant piston bowl CI engine. The analysis has been done using ECFM-3Z model of STAR-CD. Suitable modifications in the existing code are done to incorporate the HCCI mode of combustion. The ECFM -3Z model for HCCI mode of combustion is validated with the existing literature to make sure that the results obtained are accurate. The parameters like compression ratio and boost pressure are varied under different swirl ratios to analyze the rate of heat transfer in the combustion chamber. The analysis resulted in achieving maximum increased heat transfer rates of 0.88% to the wall with swirl ratio 1, 45.66% to the dome and 39.99% to the piston with swirl ratio 4; when the compression ratios are increase from 18 to 21. A maximum increase in heat transfer rates of 15.82% to the wall, 26.41% to the dome and 27.46% to the piston with compression ratio 21; when the swirl ratio is increase from 1 to 4. Similarly a maximum increased heat transfer rates of 83.75% to the wall with swirl ratio 4, 88.04% to the dome with swirl ratio 3 and 87.52% to the piston with swirl ratio 4; when the boost pressures are increase from 1 bar to 2 bar were achieved. A maximum increase in heat transfer rates of 59.35% to the wall with boost pressure 1.5 bar, 81.32% to the dome and 76.34% to the piston with boost pressure 2 bar; when the swirl ratio is increase from 1 to 4 were obtained. The study revealed that apart from adopting higher compression ratios and boost pressures adoption of high swirl ratios is observed to be contributing to a large extent in enhancing the rates of heat transfer which would lead to significant reduction in in-cylinder temperatures suitable for low NOx emission formation in HCCI mode.

**Keywords:** HCCI engine; ECFM-3Z; Rate of heat transfer; Swirl ratio; Boost pressure; Compression ratio

### 1. Introduction

IC Engines have become indispensible prime movers over the past one and half century. Though the performance of conventional SI and CI engines is satisfactory, SI engine suffers from poor part load efficiency and high CO emissions. The CI engine yields high particulate and NOx emissions. These effects may be attributed to their conventional combustion process. Of late, a hybrid combustion process called Homogeneous charge compression ignition (HCCI) equipped with advanced low-temperature combustion technology is gaining attention by researchers. In principle, HCCI involves the volumetric auto combustion of a premixed fuel, air, and diluents at low to moderate temperatures and at high compres-

sion ratios. The other associated advantages with HCCI mode of combustion have been well documented and presented as a potentially promising combustion mode for internal combustion engines [1, 2].

Swirl helps in homogeneous mixture formation of the fuel and air [3]. It also helps in NOx emission reduction [4].

The increase in swirl ratio reduces the peak temperatures by increasing the heat transfer to the combustion chamber parts.

This leads to a low temperature combustion process resulting in low NOx emissions [5]. The rate of heat transfer effecting NOx emissions was discussed in the author's previous work [6].

The heat transfer from the bulk gas to the combustion chamber in HCCI engines is one of the most important and difficult tasks in HCCI simulations since it influences the in-cylinder pressure and temperature, the fuel consumption and the pollutants. Swirl helps in homogeneous mixture formation

<sup>\*</sup>Corresponding author. Tel.: +919912194512  
E-mail address: karthikeya.sharma3@gmail.com

<sup>†</sup>Recommended by Associate Editor Jeong Park  
© KSME & Springer 2015

Table 1. Combustion models capabilities.

Model	Applicability
G-equation	Partially premixed S.I & C.I
DARS-TIF	Compression ignition
ECFM	Non-homogeneous premixed S.I.
ECFM- 3Z	Premixed and NON premixed S.I and C.I

at the same time it increases the heat transfer losses. Though increase in heat transfer losses helpful in reducing the pollutants like  $\text{NO}_x$  and CO, it also contributes to the power output loss. The reason for this is increased turbulence inside the combustion chamber with increase in swirl ratio is responsible for increase in heat transfer losses. In one way it can be considered as a forced convection heat transfer between combustion gasses and combustion chamber body parts.

Performing these explorations (under different operating parameters with induction induced swirl) solely in the laboratory would be inefficient, expensive and impractical since there are many variables that exhibit complex interaction. Because of this reason, a CFD tool Star- CD is chosen for the analysis. Several modifications were made to Star- CD es-ice module so that it could be used for HCCI engine modeling. The different combustion models which are well developed for predicting engine processes are Transient interactive flamelets (TIF) model, Digital analysis of reaction system –Transient interactive flamelets model (DARS-TIF), G –equation model [7], Extended coherent flame combustion model -3 Zones [8] and the, Equilibrium-limited ECFM (ECFM-CLEH) [9, 10]. Each model has its own limitations and is suitable for a specific set of problems. Generally speaking; ECFM-3Z and ECFM-CLEH can be used for all types of combustion regime whereas ECFM-3Z is mostly suitable for homogeneous turbulent premixed combustion with spark ignition and Compression ignition. Various combustion models applicability's are shown in Table 1. Owing to its wide applicability, in the present work ECFM- 3Z has been used to study the effect of swirl motion of intake charge on emissions and performance of HCCI engine. Fig. 1 depicts the schematic representation of the three zones of the ECFM- 3Z model. This model is capable of simulating the complex mechanisms like turbulent mixing, flame propagation, diffusion combustion and pollutant emission that characterize modern IC engines.

Induction induced swirl has a predominant effect on mixture formation and rapid spreading of the flame front in the conventional combustion process of a CI engine. This has been well documented in the literature. However, it is observed that no work has been done on the effect of swirl in HCCI mode.

The main objective of the present study is to analyze heat transfer to the combustion chamber under the induction induced swirl in a HCCI engine under varying operating parameters. Increased heat transfer rates to the parts of the combustion chamber leads to a low temperature combustion, fa-

Table 2. Engine specifications.

Engine specifications	
Displacement volume	1600 $\text{cm}^3$
Bore	12.065 cm
Stroke	14 cm
Connecting rod length	26 cm
Compression ratio	21:1
Fuel	n-Dodecane
Operating conditions	
Engine speed	1000 rpm
Equivalence ratio	0.26
Inlet temperature air ( $T_{\text{air}}$ )	353 K
Inlet air pressure ( $P_{\text{air}}$ )	0.1 MPa
Cylinder wall temperature ( $T_{\text{wall}}$ )	450 K
EGR	0%

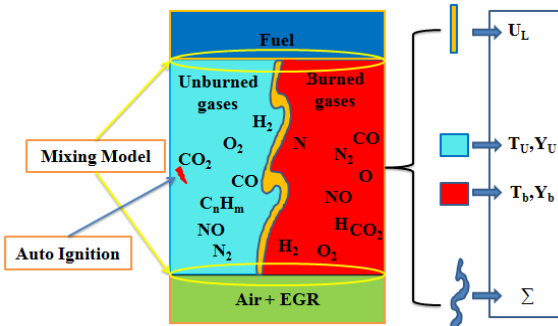


Fig. 1. Schematic representation of three zones of ECFM-3Z model.

voring low  $\text{NO}_x$  formation.

For this purpose swirl ratio is varied between 1 to 4, under different operating parameters like compression ratio and boost pressure.

## 2. Methodology

A single cylinder direct injection, reentrant piston bowl, CI engine with specifications given in Table 2 has been considered for the analysis. A CFD package STAR-CD is used with necessary modifications for the analysis to study the rates of heat transfer inside the combustion chamber with swirl and other operating parameters in CI engine HCCI Mode. The engine specifications considered for the analysis are shown in Table 2.

## 3. CFD model set- up

The computational mesh consists of 128000 cells representing 1/6<sup>th</sup> of piston bowl created in STAR-CD by generating a spline based on the piston bowl shape. A 2D template was cut by the spline to cut the 3D mesh with 40

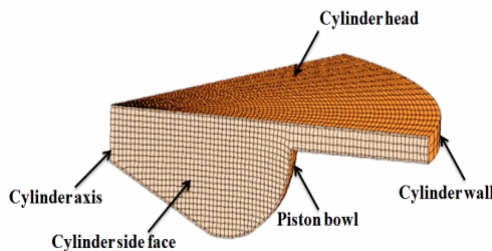


Fig. 2. Schematic representation of 3D piston bowl shape at TDC.

radial cells, 160 axial cells, 5 top dead center layers and 40 axial block cells. The piston bowl shape and 3D mesh of the piston bowl sector is shown in Fig. 2.

Energy efficiency of the engine is analyzed by gross indicated work per cycle (W) calculated from the cylinder pressure and piston displacement using Eq. (1):

$$W(\text{Nm}) = \frac{\pi a B_2}{8} \int_{\theta_1}^{\theta_2} p(\theta) \left[ 2 \sin(\theta) \frac{\text{asin}(2\theta)}{\sqrt{l^2 - a^2 \sin^2(\theta)}} \right] d\theta \quad (1)$$

where  $a$ ,  $l$  and  $B$  are the crank radius, connecting rod length and cylinder bore, respectively, and  $\theta_1$  and  $\theta_2$  are the beginning and the end of the valve-closing period.

The indicated power per cylinder (P) is related to the indicated work per cycle by using Eq. (2):

$$P(\text{kW}) = \frac{WN}{60000n_R} \quad (2)$$

where  $n_R = 2$  is the number of crank revolutions for each power stroke per cylinder and  $N$  is the engine speed (rpm). The Indicated specific fuel consumption (ISFC) is shown in Eq. (3):

$$\text{ISFC}(\text{g/kWh}) = \frac{30m_{\text{fuel}}N}{P} \quad (3)$$

In Eq. (1), the power and ISFC analyses can be viewed as being only qualitative rather than quantitative in this study.

#### 4. Modeling strategy

The STAR-CD used in the present study has integrated several sub models such as turbulence, fuel spray and atomization, wall function, ignition, combustion, NOx, and soot models for various types of combustion modes in CI as well as SI engine computations. As initial values of  $k$  and  $\varepsilon$  are not known priori the turbulence initialization is done using I-L model. For this purpose local turbulence intensity,  $I$ , and length scale,  $L$ , are related as

$$k_\infty = 3/2 I^2 V_\infty^2 \quad (4)$$

$$\varepsilon_\infty = C^{3/4} \mu (k_\infty)^{3/2} / L \quad (5)$$

This practice will ensure that  $k$  and  $\varepsilon$  and the turbulent viscosity  $\mu_t$  will all scale correctly with  $V_\infty$ , which is desirable from both the physical realism and numerical stability point of view. Moreover the turbulent intensity is defined using the same velocity vector magnitude as that of stagnation quantities.

The combustion is modeled using ECFM-3Z. As far as fluid properties are concerned, ideal gas law and temperature dependent constant pressure specific heat ( $C_p$ ) are chosen.

The ECFM-3Z incorporates the following models in its operation.

#### Phenomena --- Model

- Spray injection and Atomization---Huh (1991)
- Auto Ignition model---Double delay auto ignition
- Combustion---ECFM-3Z Compression Ignition (Colin and Benkenida (2004))
- Turbulence---Intensity-Length scale
- Droplet breakup---Reitz-Diwakar (1986)
- Liquid Film---Angelberger et al (1997)
- Droplet wall interaction---Bai and Gosman (1996)
- Boiling ---Rohsenow (1952)
- NOx---Extended Zel'dovich mechanism
- Soot---Mauss, Karlson (2006).

#### 5. Initial and boundary conditions

The initial boundary conditions considered for the analysis are; an absolute pressure of 1.02 bar, 353 K initial temperature, 0% EGR, 0.26 equivalence ratio. Wall temperatures of combustion dome region are fixed as 400 K, dome regions as 450 K and piston crown regions as 450 K. The Angleberger wall function mode [11] is considered. By solving momentum, turbulence and mass equations boundary layers with no-slip are computed by 'two-layer' and low Reynolds number approaches. In the analysis a combined "two layered" and "low Reynolds number" hybrid wall boundary condition is used. The need for using a small value for  $y^+$  was eliminated by the use of hybrid wall boundary condition, which creates very fine mesh near the walls. By using the expression of asymptotic valid for  $0.1 < y^+ < 100$  or by combining the low and high Reynolds number expression for chemical species, thermal energy, shear stresses wall fluxes the  $y^+$  independency was achieved along with providing all necessary boundary conditions for a wide range of near-wall mesh densities. The variable values on the wall and at the near wall cells are calculated by using hybrid wall functions.

#### 6. Validation of ECFM-3Z

STAR-CD is a well known Commercial CFD package being adopted many renowned researchers and well established research organizations in the field of automotive IC engines. The results obtained through this package are validated with

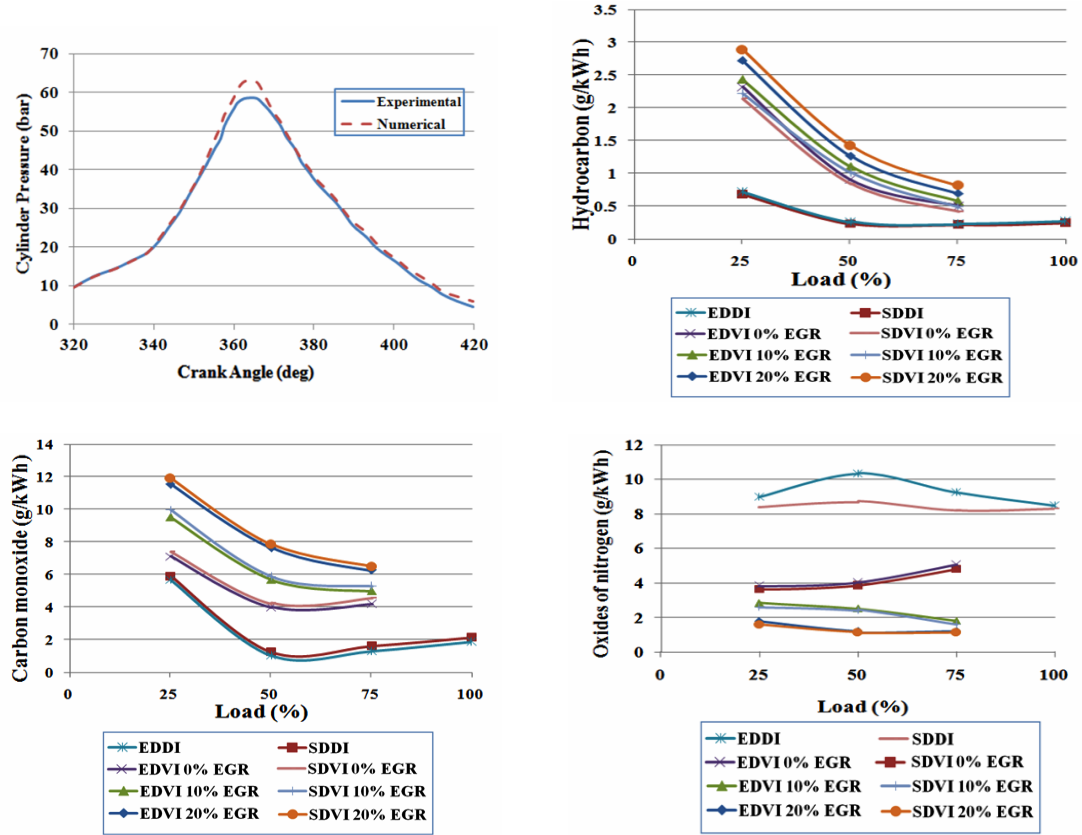


Fig. 3. Validation of the ECFM-3Z Compression ignition model with the experimental results of External mixture formation of HCCI engine.

the experimental results by many authors like Pasupathy Venkateswaran [12] et al., Zellat Marc et al. [13], Bakhshian et al. [14]. A comparison of the CI engine in HCCI are done in this paper considering the extended coherent flame combustion three zones, compression model for combustion analysis. The present paper deals with the simulation of CI engine in HCCI mode, using a fuel vaporizer to achieve excellent HCCI combustion in a single cylinder air-cooled direct injection diesel engine. No modifications were made to the combustion system. Ganesh et al. [15] conducted experiments with diesel vapor induction without EGR and diesel vapor induction with 0%, 10% and 20% EGR. Validation of the present model with the experimental results of Ganesh et al. [15] was done by considering all the engine specifications.

Ganesh et al. [15] considered a vaporized diesel fuel with air to form a homogeneous mixture and inducted into the cylinder during the intake stroke. To control the early ignition of diesel vapor-air mixture, cooled (30°C) Exhaust gas recirculation (EGR) technique was adopted. For the validation purpose, the results are compared with respect to engine performance and emissions in the following figures. It is observed that the simulated results are in good agreement with the experimental results. The comparison of the plots between simulation and experimental results are shown in the Fig. 3. In the figures EDVI represents the experimental diesel vapor injec-

tion and SDVI represents simulated diesel vapor induction at respective EGR concentrations.

## 7. Results and discussion

In the present paper the effect of induced swirl and other operating parameters like compression ratio and boost pressure on the heat transfer rate is studied. The swirl ratios ranging from 1 to 4 are considered for the analysis. The simulation results of the ECFM-3Z model are discussed below.

### 7.1 Heat transfer to the piston vs compression ratio

The variation of heat transfer to the piston with compression ratio for swirl ratios 1 to 4 is plotted in Fig. 4. From Table 3, it can be observed that higher compression ratios and higher swirl ratios are favorable in increasing the heat transfer to piston. The heat transfer rates obtained at different compression ratios and swirl ratios are summarized in Table 3. The heat transfer to the piston increases with increase in compression ratio irrespective of the swirl ratio, but the percentage increase in heat transfer is less at low swirl ratios and more at high swirl ratios. As swirl ratio increases; increased heat transfer rates are obtained at all compression ratios, but the increase in heat transfer rates are high at higher compression ratios.

Table 3. Heat Transfer to the piston (W) at various compression ratios and swirl ratios.

Compression ratio piston	SW1	SW2	SW3	SW4	Percentage increase between SW1-SW4
CR 18	-497.279	-534.548	-572.621	-605.147	21.69
CR19	-559.89	-600.553	-642.503	-668.234	19.35
CR20	-604.907	-653.655	-703.826	-760.625	25.74
CR 21	-664.658	-720.865	-780.307	-847.185	27.46
Percentage increase between CR 18-CR21	33.65	34.85	36.26	39.99	

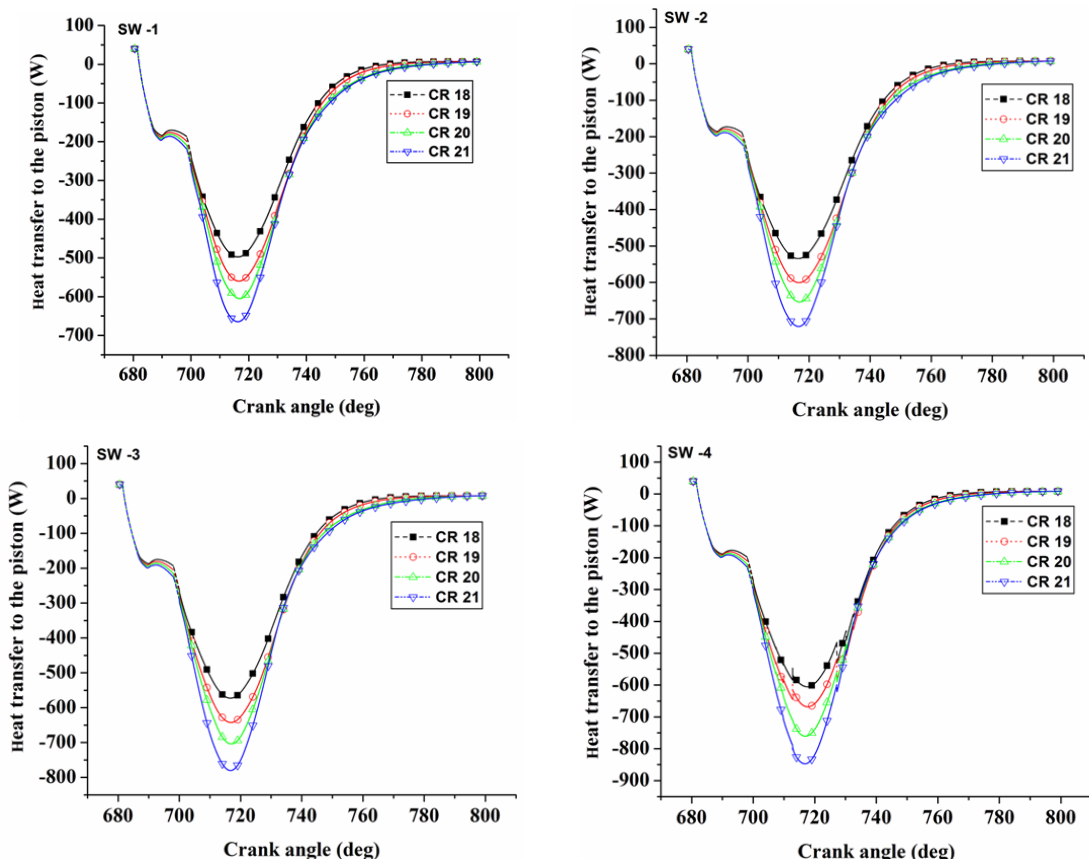


Fig. 4. Heat transfer to the piston vs Crank angle at different compression ratios and swirl ratios.

The reason for this phenomenon is increase in turbulence owing to increased wall heat transfer due to increased swirl intensity.

### 7.2 Heat transfer to the walls vs compression ratio

The variation of heat transfer to the walls with compression ratio for swirl ratios 1to 4 is plotted in Fig. 5. The heat transfer From Table 4, it can be observed that higher compression ratios and higher swirl ratios are favorable in increasing the heat transfer to the walls [16].

The rate of heat transfer to the walls decreases with increase in compression ratio irrespective of the swirl ratio, but the percentage decrease in heat transfer is high at lower swirl ra-

tios and less at higher swirl ratios. As swirl ratio increases; increased heat transfer rates are obtained at all compression ratios, but the increase in heat transfer rates are high at higher compression ratios. The reason for this phenomenon is increase in turbulence owing to increased wall heat transfer due to increased swirl intensity and increases in compression increases the combustion chamber temperatures this increases the heat transfer at higher compression ratios when compared with lower swirl ratios.

### 7.3 Heat transfer to the piston vs boost pressure (BP)

The variation of heat transfer to the piston with boost pressure for swirl ratios 1to 4 is plotted in Fig. 7. From Table 6, it

Table 4. Heat transfer to the piston (W) at various compression ratios and swirl ratios.

Wall	SW1	SW2	SW3	SW4	Percentage increase between SW1-SW4
CR 18	-101.424	-104.492	-107.676	-113.738	12.14
CR 19	-99.4872	-102.53	-105.736	-111.741	12.31
CR 20	-97.7564	-100.806	-103.903	-109.828	12.34
CR 21	-97.323	-100.373	-103.454	-112.726	15.82
Percentage reduction between CR 18-CR 21	4.04	3.94	3.92	0.88	

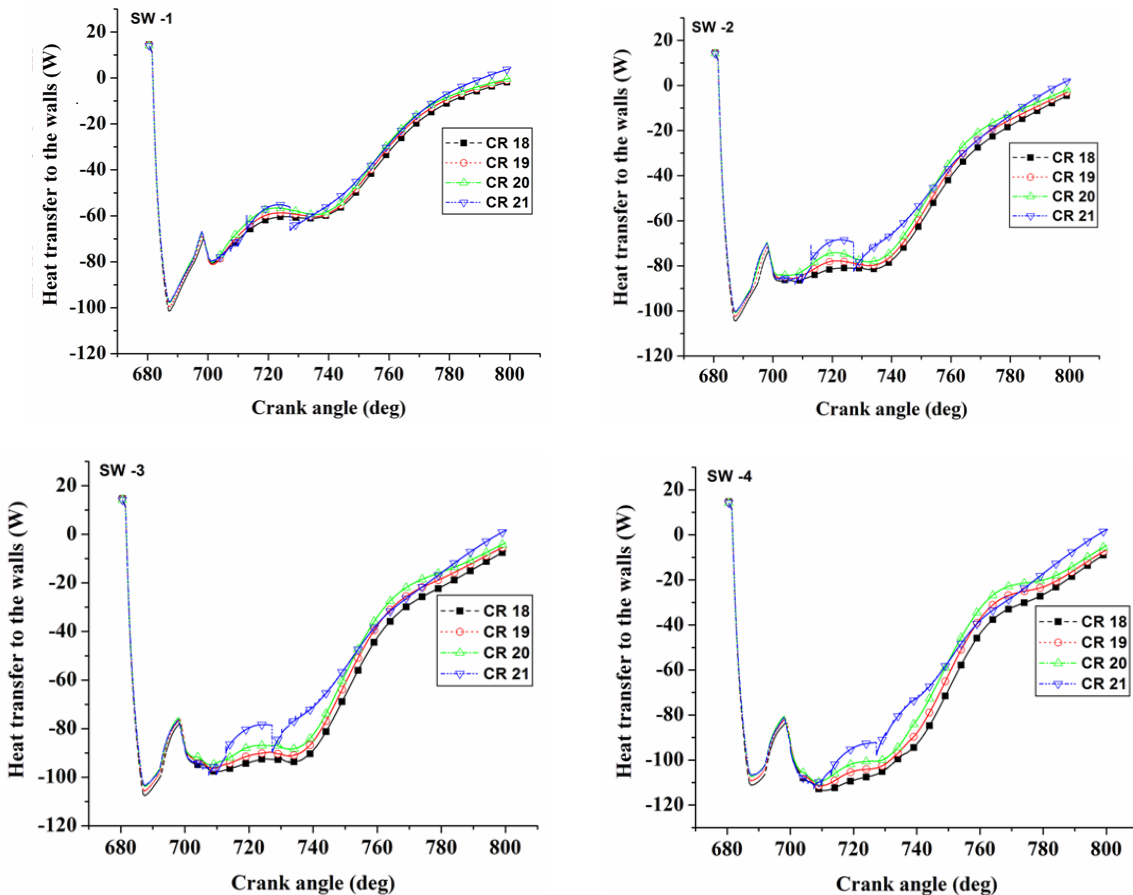


Fig. 5. Heat transfer to the walls vs Crank angle at different compression ratios and swirl ratios.

can be observed that higher boost pressures and higher swirl ratios are favorable in increasing the heat transfer to piston.

The heat transfer rates obtained at different boost pressures and swirl ratios are summarized in Table 6. The heat transfer to the piston increases with increase in boost pressure irrespective of the swirl ratio, but the percentage increase in heat transfer is high at high swirl ratios. As swirl ratio increases; increased heat transfer rates are obtained at all boost pressures, but the increase in heat transfer rates are high at higher compression ratios [17]. The reason for this phenomenon is increase in turbulence owing to increased wall heat transfer due to increased swirl intensity.

#### 7.4 Heat transfer to the walls vs boost pressure

The variation of heat transfer to the walls with boost pressure for swirl ratios 1 to 4 is plotted in Fig. 8. The heat transfer rates obtained at different boost pressures and swirl ratios are summarized in Table 7. From Table 7, it can be observed that higher boost pressures and higher swirl ratios are favorable in increasing the heat transfer to the walls [18]. The heat transfer to the walls increases with increase in boost pressure irrespective of the swirl ratio, but the percentage increase in heat transfer is high at higher swirl ratios. As swirl ratio increases; increased heat transfer rates are obtained at all boost pressures,

Table 5. Heat transfer to the dome (W) at various boost pressures and swirl ratios.

BP (bar) Piston	SW1	SW2	SW3	SW4	Percentage increase between SW1-SW4
BP 1.0	-605.147	-668.234	-760.625	-847.185	39.99
BP 1.25	-695.316	-783.45	-921.533	-870.235	25.15
BP 1.5	-786.091	-909.186	-1086.87	-1230.32	56.51
BP 1.75	-843.802	-1052.96	-1249.11	-1413.43	67.50
BP 2.0	-900.895	-1173.55	-1401.41	-1588.69	76.34
Percentage increase between BP 1.0-BP 2.0	48.87	75.61	84.24	87.52	

Table 6. Heat transfer to the walls (W) at various boost pressures and swirl ratios.

BP (bar) Wall	SW1	SW2	SW3	SW4	Percentage increase between SW1-SW4
BP 1.0	-97.323	-100.373	-103.454	-112.726	15.82
BP 1.25	-108.397	-111.858	-115.963	-127.434	17.56
BP 1.5	-112.6852	-121.664	-134.296	-179.592	59.37
BP 1.75	-125.707	-130.442	-154.338	-183.404	45.89
BP 2.0	-132.643	-146.525	-175.965	-207.142	56.16
Percentage increase between BP 1.0-BP 2.0	36.29	45.98	70.09	83.75	

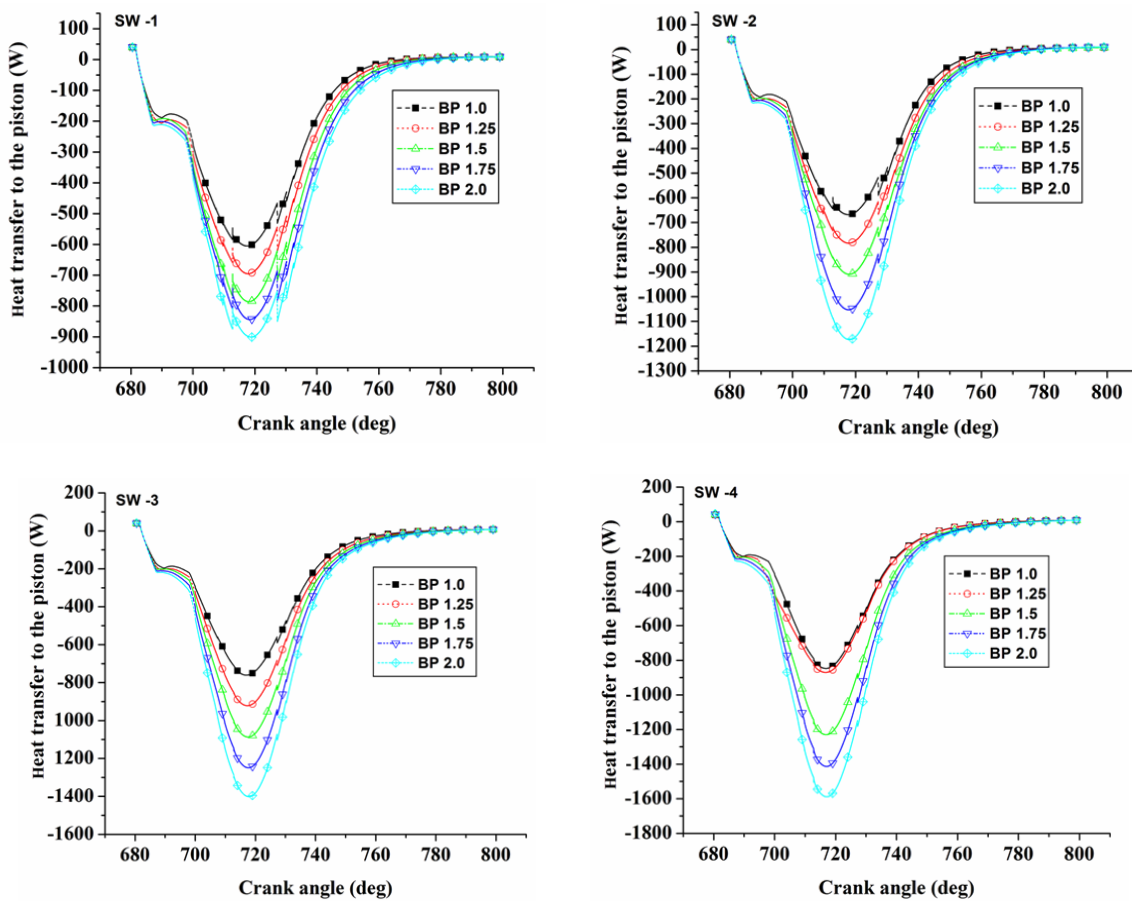


Fig. 6. Heat transfer to the piston vs Crank angle at different boost pressures and swirl ratios.

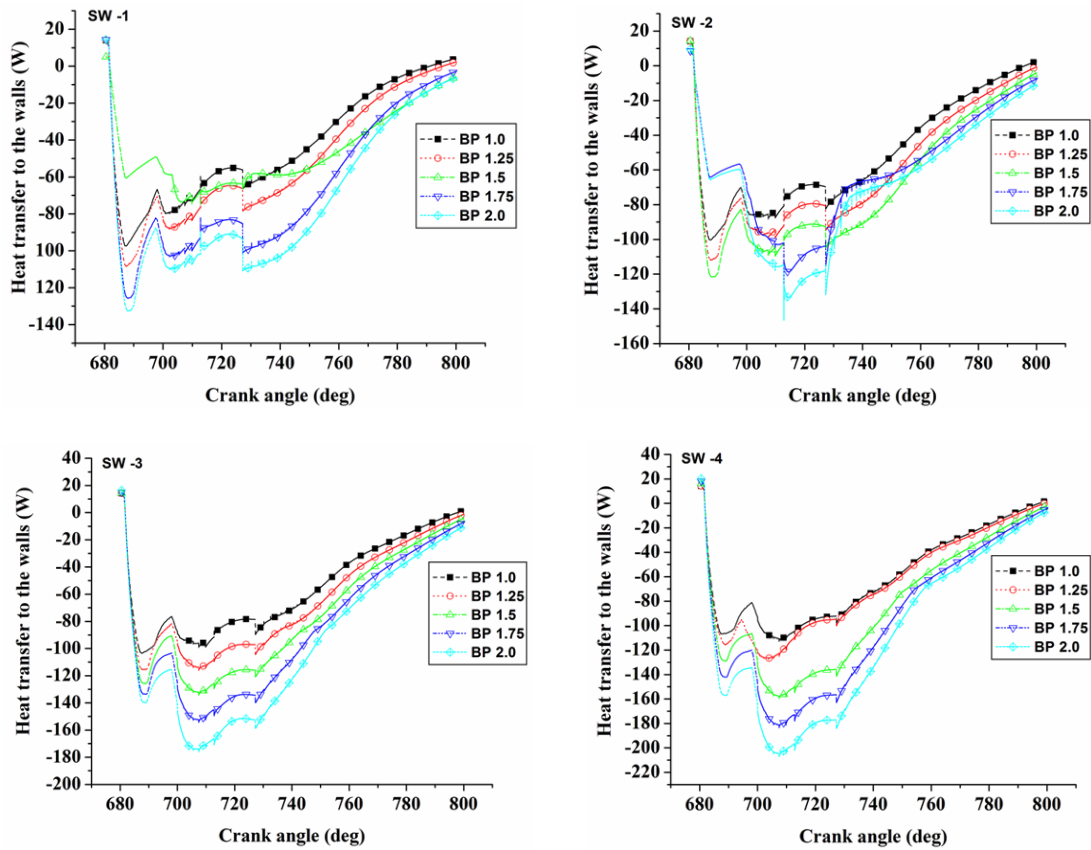


Fig. 7. Heat transfer to the walls vs Crank angle at different boost pressures and swirl ratios.

but the increase in heat transfer rates are high at boost pressure 1.5 bar. The reason for this phenomenon is increase in turbulence owing to increased wall heat transfer due to increased swirl intensity and increases in boost pressure increases the combustion chamber temperatures this increases the heat transfer at higher boost pressures when compared with lower swirl ratios.

## 8. Conclusions

The present study revealed that ECFM-3Z of STAR-CD is well suitable for predicting HCCI mode of combustion with necessary modifications, in coherence with the existing literature. It was found that swirl ratio has a considerable impact in increasing the heat transfer rates in a HCCI engine.

The analysis resulted in achieving maximum increased heat transfer rates of 0.88% to the wall with swirl ratio 1, 45.66% to the dome and 39.99% to the piston with swirl ratio 4; when the compression ratios are increase from 18 to 21. A maximum increase in heat transfer rates of 15.82% to the wall, 26.41% to the dome and 27.46% to the piston with compression ratio 2; when the swirl ratio is increase from 1 to 4. Similarly a maximum increased heat transfer rates of 83.75% to the wall with swirl ratio 4, 88.04% to the dome

with swirl ratio 3 and 87.52% to the piston with swirl ratio 4; when the boost pressures are increased from 1 bar to 2 bar were achieved. A maximum increase in heat transfer rates of 59.35% to the wall with boost pressure 1.5 bar, 81.32% to the dome and 76.34% to the piston with boost pressure 2 bar; when the swirl ratio is increased from 1 to 4 were obtained. The effect of the operating parameters viz; compression ratio and boost pressures under varying swirl ratios suggested higher swirl ratios, higher compression ratios and boost pressures are favorable to increase the rate of heat transfer to the parts of the combustion chamber leading to low NOx formation conditions. The study revealed that apart from adopting higher compression ratios and boost pressures adoption of high swirl ratios is observed to be contributing to a large extent in enhancing the rates of heat transfer which would lead to significant reduction in in-cylinder temperatures suitable for low NOx emission formation in HCCI mode.

## Acknowledgements

The authors thank Dr.Raja Banerjee, Associate Professor, IIT Hyderabad for allowing to use computational facility, Mr.B.Siva Nageswara Rao from CD-adapco, Bengaluru and Mr.P.Madhu computer Lab supervisor IIT Hyderabad for their

support during the simulation work.

## References

- [1] K. Epping, S. M. Aceves, R. L. Bechtold and J. E. Dec, The potential of HCCI combustion for high efficiency and low emissions, *SAE Paper No. 2002-01-1923*.
- [2] T. K. Sharma, G. A. P. Rao and K. Madhumurthy, Combustion analysis of ethanol in HCCI engine, *Trends in Mech. Engg.*, 3 (1) (2012).
- [3] R. Manimaran and R. T. K. Raj, Computational studies of swirl ratio and injection timing on atomization in a direct injection diesel engine, *Front. in Heat & Mass Trans. (FHMT)*, 5 (1) (2014).
- [4] S. P. Venkateswaran and G. Nagarajan, Effects of the re-entrant bowl geometry on a DI turbocharged diesel engine performance and emissions—A CFD approach, *J. Engg. for Gas Turb. and Power*, 132 (12) (2010) 122803.
- [5] F. Maroteaux, L. Noel and A. Ahmed, Numerical investigations on methods to control the rate of heat release of HCCI combustion using reduced mechanism of n-heptane with a multidimensional CFD code, *Comb. Theory and Model*, 11 (4) (2007) 501-525.
- [6] T. K. Sharma, G. A. P. Rao and K. Madhumurthy, Effect of swirl of performance and emissions of CI engine in HCCI mode, *J. Braz. Soc. Mech. Sci. Eng.*, 37 (2015) 1405-1416.
- [7] J. M. Duclos, M. Zolver and T. Baritaud, 3D modeling of combustion for DI-SI engines, *Oil & Gas Sci & Tech – Rev. IFP*, 54 (2) (1999) 259-264.
- [8] O. Colin and A. Benkenida, The 3-zone extended coherent flame model (ECFM3Z) for computing premixed/diffusion combustion, *Oil & Gas Sci & Tech – Rev. IFP*, 59 (6) (2004) 593-609.
- [9] F. Ravet, D. Abouri, M. Zellat and S. Duranti, Advances in combustion modeling in STAR-CD: Validation of ECFM CLE-H model to engine analysis, *18th Int. Multid Eng Users' Meet SAE Congress*, Detroit, April, 13 (2008).
- [10] G. Subramanian, L. Vervish and F. Ravet, New developments in turbulent combustion modeling for engine design: ECFM-CLEH combustion sub model, *SAE Int. - 2007-01-0154*.
- [11] V. Moureau, G. Lartigue, Y. Sommerer, C. Angelberger, O. Colin and T. Poinsot, Numerical methods for unsteady compressible multi-component reacting flows on fixed and moving grids, *Int J. Comput. Phys.*, 202 (2) (2005) 710-736.
- [12] S. P. Venkateswaran and G. Nagarajan, Effects of the re-entrant bowl geometry on a DI turbocharged diesel engine performance and emissions—A CFD approach, *J. Engg. Gas Turb. and Power*, 132 (12) (2010).
- [13] M. Zellat et al., Towards a universal combustion model in STAR-CD for IC engines: from GDI to HCCI and application to DI Diesel combustion optimization, *Proc. 14th Int. Multid. Eng. User's Meeting*, SAE Cong. (2005).
- [14] Y. Bakhshan et al., Multi-dimensional simulation of n-heptane combustion under HCCI engine condition using detailed chemical kinetics, *The J. Eng. Research*, 22 (2011).
- [15] D. Ganesh and G. Nagarajan, Homogeneous charge compression ignition (HCCI) combustion of diesel fuel with external mixture formation, *Energy*, 35 (1) (2010) 148-157.
- [16] E. Neshat and R. K. Saray, Effect of different heat transfer models on HCCI engine simulation, *Energy Conversion and Management*, 88 (2014) 1-14.
- [17] M. T. García, F. J. J.-E. Aguilar, T. S. Lencero and J. A. B. Villanueva, A new heat release rate (HRR) law for homogeneous charge compression ignition (HCCI) combustion mode, *Applied Thermal Engineering*, 29 (17) (2009) 3654-3662.
- [18] M. Christensen and B. Johansson, Per Amnéus and Fabian Mauss, Supercharged homogeneous charge compression ignition. *SAE Technical paper*, No. 980787 (1998).



**T. Karthikeya Sharma** is the Research Scholar, Dept. of Mechanical Engineering, NIT Warangal, India. He did masters from JNTU Anantapur and Graduated from GPREC Kunrool. His areas of interest are IC Engines, Engine simulation.



**G. Amba Prasad Rao** is working as a Professor in Dept. of Mechanical Engineering, NIT Warangal-506 004, India. His total teaching experience is 25 years. His areas of interest are IC Engines, Alternate Fuels, Emissions and its control, Engine simulation.



**K. Madhu Murthy** is working as a Professor in Dept. of Mechanical Engineering, NIT Warangal-506 004, India. His total teaching experience is 30 years. His areas of interest are IC Engines, Emissions control, Industrial Management, and entrepreneurship.